molecular systems biology

A pharmaco-epistasis strategy reveals a new cell size controlling pathway in yeast

Fabien Moretto[1,2], Isabelle Sagot[1,2], Bertrand Daignan-Fornier[1,2,*] and Benoît Pinson[1,2]

[1] Université Bordeaux, IBGC, UMR 5095, Bordeaux, France and [2] Institut de Biochimie et Génétique Cellulaires, CNRS UMR 5095, Bordeaux, France
* Corresponding author. Institut de Biochimie et Génétique Cellulaires, CNRS UMR 5095, 1, rue Camille Saint Saëns, 33077 Bordeaux Cedex, France.
Tel.: +33 556 999 001; Fax: +33 556 999 059; E-mail: B.Daignan-Fornier@ibgc.cnrs.fr

Cell size is a complex quantitative trait resulting from interactions between intricate genetic networks and environmental conditions. Here, taking advantage of previous studies that uncovered hundreds of genes affecting budding yeast cell size homeostasis, we performed a wide pharmaco-epistasis analysis using drugs mimicking cell size mutations. Simple epistasis relationship emerging from this approach allowed us to characterize a new cell size homeostasis pathway comprising the sirtuin Sir2, downstream effectors including the large ribosomal subunit (60S) and the transcriptional regulators Swi4 and Swi6. We showed that this Sir2/60S signaling route acts independently of other previously described cell size controlling pathways and may integrate the metabolic status of the cell through NAD^+ intracellular concentration. Finally, although Sir2 and the 60S subunits regulate both cell size and replicative aging, we found that there is no clear causal relationship between these two complex traits. This study sheds light on a pathway of >50 genes and illustrates how pharmaco-epistasis applied to yeast offers a potent experimental framework to explore complex genotype/phenotype relationships.

Introduction

Cell size, similar to the majority of phenotypic characters, is the result of complex genetic interactions. Cell size can vary substantially across cell types and organisms. It is influenced by endogenous factors such as ploidy but also by environmental conditions. However, for a given cell type in a defined growth condition, cell volume distribution is constant, thus arguing for a homeostatic control of cell size (Jorgensen and Tyers, 2004). Preserving cell size homeostasis necessitates gauging cell size and coordinating growth (increase in volume) and proliferation (increase in cell number). In unicellular organisms such as bacteria or yeast, cell size drastically varies with the richness of the medium (Wright and Lockhart, 1965; Johnston *et al*, 1979), implying a supplementary level of cell size regulation herein referred to as 'nutrient control'. In fact, cells grown in poor media are significantly smaller than those grown in rich media (Johnston *et al*, 1979). Two major non-exclusive hypotheses have been proposed to account for nutrient control of cell size. First, decreasing cell size leads to an increase of the cell surface to volume ratio and could, therefore, be advantageous for the uptake of scarce nutrients (Hennaut *et al*, 1970; Adams and Hansche, 1974). Second, diminishing cell size minimizes the amount of biomass needed for each division round and, therefore, allows the increase of cell number before complete starvation

(Jorgensen *et al*, 2004; Jorgensen and Tyers, 2004). In both scenarios, cell size regulation by nutrients would contribute to an increased fitness of the population under sub-optimal conditions.

In microorganisms, nutrient control of cell size has been studied for decades. In *Bacillus subtilis* (Weart *et al*, 2007), it has been shown that nutrient control of cell size occurs through a mechanism involving a metabolic enzyme (the glucosyltransferase UgtP), which, together with its substrate (UDP-glucose), inhibits cell division. This elegant work has provided the first mechanism connecting a specific metabolic activity to the control of cell size and proliferation. In budding yeast, the key notion of 'critical size' has emerged, defined as the minimal size required for entering a new cell division cycle (Hartwell *et al*, 1974; Johnston *et al*, 1977). Although the averaged 'critical size' is relatively constant in a defined culture condition, it varies with the nutrient content of the medium (Johnston *et al*, 1979). How yeast cells convert a 'sufficient biomass signal', which could reflect volume, mass and/or biosynthetic capacity, into a 'division signal' is not entirely understood. Genetic approaches have been widely used to identify the key factors in this process. The first characterized mutants with a reduced cell size (named *whi*) affected the cyclin Cln3p. Although alleles of *CLN3* stabilizing the protein lead to cell size diminution (Carter and Sudbery, 1980; Sudbery *et al*, 1980; Nash *et al*, 1988), knockout of *CLN3*

leads to a cell size increase (Lew *et al*, 1992). Cln3p interacts with the cyclin-dependent kinase Cdc28p and inhibits Whi5p, a Rb homolog that negatively regulates the MBF (Swi6/Mbp1) and SBF (Swi6/Swi4) transcription activators (Costanzo *et al*, 2004; de Bruin *et al*, 2004). Thereby, Cln3p/Cdc28p stimulates the transcriptional activation of >100 genes involved in the transition from G1 to S phase (Spellman *et al*, 1998). However, Cln3 is not essential for cell cycle progression, possibly because of a partial functional redundancy with Bck2 (Ferrezuelo *et al*, 2009). The precise function of Bck2 is unclear, but this protein contributes to the activation of many genes, including most of Cln3 targets (Ferrezuelo *et al*, 2009). Together, these results pointed to the G1/S transition machinery as a major factor in cell size regulation, yet other cell cycle regulators could also have a role in cell size homeostasis (Harvey and Kellogg, 2003). In a reciprocal way, cell size control contributes to G1 length variability (Goranov and Amon, 2010). Moreover, cell growth capacity varies with cell cycle position, this capacity being higher in G1 and anaphase than during other cell cycle stages (Goranov *et al*, 2009). Recently, Polymenis and coworkers (Hoose *et al*, 2012) further substantiated the complex relations between cell cycle progression and cell size control by reporting that many mutations disturbing cell cycle progression do not affect cell size. Therefore, our understanding on how the upstream 'cell size signals' are conveyed and integrated to the control of cell cycle progression remains to be clarified.

Systematic identification of yeast cell size mutants, using knockout collections, has revealed the complexity of cell size homeostasis pathways (Jorgensen *et al*, 2002; Zhang *et al*, 2002a). Indeed, these authors identified hundreds of mutants with a median cell volume diverging significantly from that of the isogenic wild type. These large-scale approaches have revealed new master regulators (Sch9p and Sfp1p) and have pointed to a central role for ribosome biogenesis and general nutrient sensing pathways (Ras and Tor) in the regulation of cell size homeostasis (Jorgensen *et al*, 2004). However, although important regulators have been well characterized, the vast majority of the identified cell size mutants, either small (*whi*) or large (*lge* and *uge*), have not yet been positioned into defined signaling pathways. Cell size control is thus a very interesting situation, where multiple loci contributing to a complex quantitative trait have been identified, but their organization into a network and their individual and combined influence remain to be elucidated.

In this study, we used a large-scale pharmaco-epistasis approach, which allowed us to characterize a new pathway containing >50 genes and responding to a metabolic signal identified as NAD^+ or a derivative. Effectors in the pathway include the sirtuin Sir2, the ribosome large subunit 60S and the transcription factors Swi4 and Swi6. Interaction with previously described master regulators, as well as intrinsic and extrinsic signals such as ploidy or medium richness, was evaluated in order to arrange this pathway within the known cell size controlling network.

Results

Cell size homeostasis is modulated by Sir2

Searching for compounds that affect yeast median cell volume (hereafter referred to as 'cell size'), we observed that nicotinamide (Nam) treatment of a wild-type strain resulted in cell size increase (Figure 1A and B). Nam, the amide form of
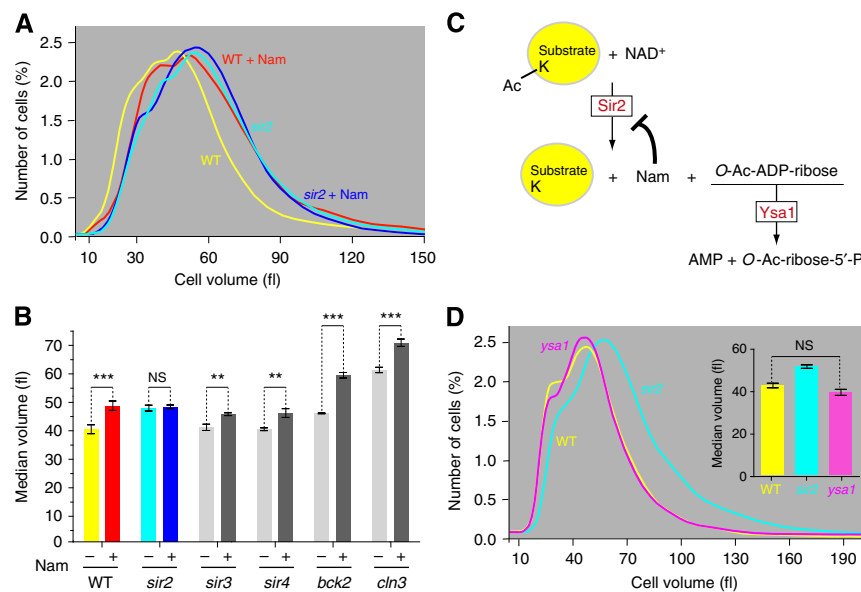

Figure 1 Cell size homeostasis is impaired in a *sir2* mutant. (**A**) Wild-type (BY4742) and *sir2* cell volume distributions. Strains were kept in exponential phase in SDcasaU medium for 48 h and then treated for 8 h with + Nam (100 μM). For each strain, cell volume distributions were determined on at least 2×10^4 cells. (**B**) Mean of median cell volumes obtained for wild type (BY4742) and mutant strains grown as in A. (**C**) Schematic representation of Sir2 and Ysa1 enzymatic activities. *O*-Ac-ADP-ribose and *O*-Ac-ribose-5′-P stand for and 2′-*O*-acetyl-adenosine diphosphate-ribose and 2′-*O*-acetyl ribose 5′-phosphate, respectively. Protein names are written in red. (**D**) The *ysa1* mutant has a wild-type cell volume. Characteristic cell volume distributions and corresponding median volumes (inset) obtained on cells grown as in A. Median volumes presented in **B** and **D** correspond to the mean of at least three independent determinations. Error bars indicate variations to the mean. Statistical analyses (**B** and **D**) correspond to an unpaired Student's *t*-test (*** $P < 10^{-3}$; ** $P < 10^{-2}$; NS, not significantly different; GraphPad Prism).

nicotinic acid (Na), inhibits the sirtuin Sir2 (Bitterman *et al*, 2002). Accordingly, we found that deleting *SIR2* caused an ∼20% increase of the cell size, as previously reported in Yang *et al* (2011), just as did a Nam treatment on wild-type cells (Figure 1A and B). Further, Nam had no effect on *sir2*Δ cell size (Figure 1A and B), thus demonstrating that Nam affects cell size through Sir2, most probably by inhibition of its enzymatic activity. As expected, the *sir2*Δ large phenotype was rescued by the *SIR2* gene reintroduced on a centromeric plasmid (Supplementary Figure 1). Nam is one of the two byproducts of the deacetylation reaction catalyzed by Sir2, the other reaction product being *O*-acetyl-ADP-ribose (Figure 1C). The *ysa1* mutant, known to accumulate *O*-acetyl-ADP-ribose (Lee *et al*, 2008), displayed a wild-type cell volume (Figure 1D). Therefore, *O*-acetyl-ADP-ribose does not seem to be involved in cell size homeostasis.

Sir2 is a histone deacetylase involved in chromatin silencing (Guarente, 1999) at specific loci together—or not—with Sir3 and Sir4. Yet, deletion of *SIR3* or *SIR4* did not affect cell size, and *sir3* or *sir4* cells were fully responsive to Nam (Figure 1B), thus showing that the effect of Sir2 on cell size is independent of Sir3 or Sir4. Importantly, unlike *sir2*Δ, other large mutants such as *cln3*Δ or *bck2*Δ were further enlarged in response to Nam (Figure 1B), thus indicating that a maximal cell size had not been reached. Accordingly, Amon and coworkers (Goranov *et al*, 2009) have shown that *Saccharomyces cerevisiae* cells can reach a cell volume as big as 800 fl. We conclude that Nam affects cell size by phenocopying the *sir2* deletion.

Mutants impairing ribosome biogenesis are epistatic to *sir2*

We then wanted to determine the genetic network through which Sir2 acts on cell size control. In order to identify downstream genetic effectors, we performed a large-scale epistasis analysis to identify small size (*whi*) mutants masking the effect of *sir2* on cell size. As the *sir2* mutants is mating deficient (Wang *et al*, 2008), the combination of *sir2* with *whi* mutations could hardly be done by large-scale mating and sporulation methods such as those developed for Synthetic Genetic Array (SGA) analysis (Tong *et al*, 2001). Instead, we took advantage of the fact that Nam affects cell size similarly to the *sir2* knockout and that the effect of Nam is totally dependent on Sir2 (Figure 1A). As Nam phenocopied the lack of Sir2, we used this drug to perform a pharmaco-epistasis analysis on 189 previously identified small size (*whi*) mutants (corresponding to the smallest mutants identified by Tyers and coworkers (Jorgensen *et al*, 2002)).

Among the 189 mutants, 22 mutants were clearly not affected by Nam (0.95 < Nam treated/untreated ratio < 1.05; Figure 2A red dots and Supplementary Table 1), indicating that these mutants act downstream of Sir2 in the pathway. Of note, we found that several mutants described as *whi* by Tyers and coworkers (Jorgensen *et al*, 2002) were larger than wild type. This most probably reflects the differences in growth conditions used between the two studies. The pharmaco-epistasis relationship was confirmed by classical genetics. We combined *sir2* deletion with 2 of the 22 mutants, *rpl35b* (Figure 2B)
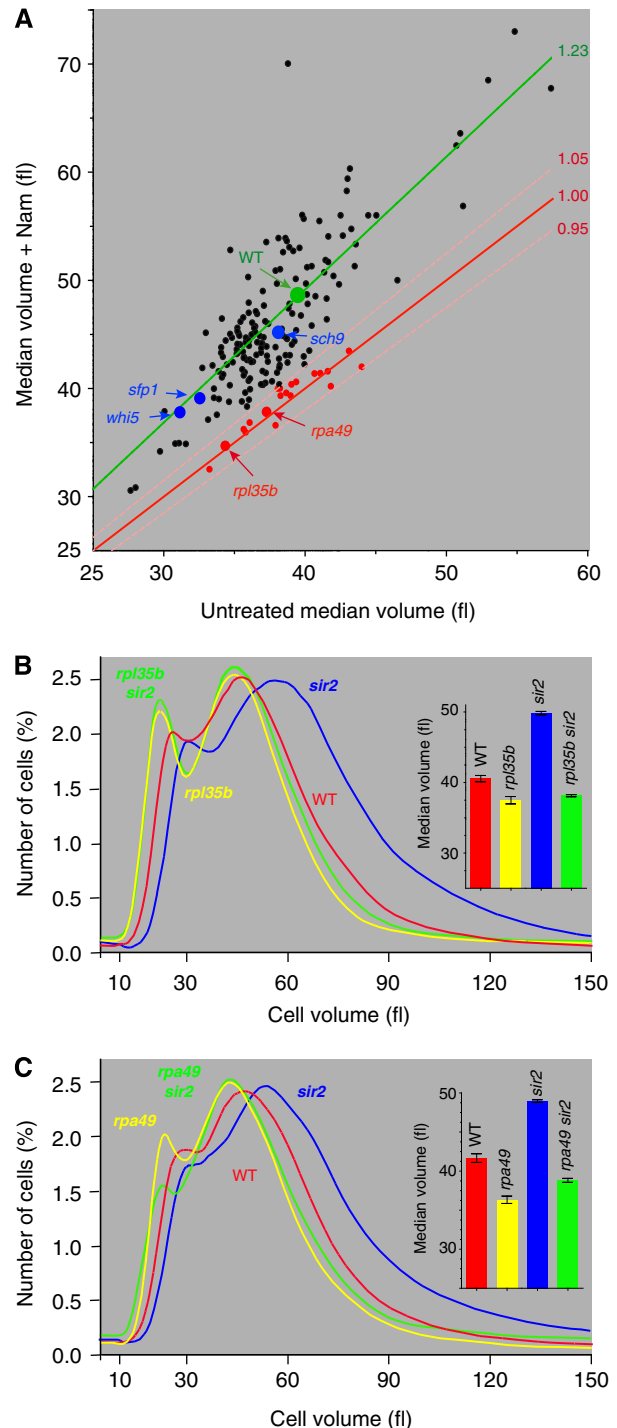

Figure 2 Mutants unaffected by Nam treatment correspond to genes mainly implicated in ribosomal biogenesis. (**A**) Median volume of various *whi* mutants treated (*y* axis) or not (*x* axis) with Nam (100 μM) as in Figure 1A. Red dots correspond to Nam-unresponsive mutants (0.95 < median volume ratio +Nam/ −Nam < 1.05), whereas green (WT), black (*whi* mutants) and blue (*sch9*, *sfp1* and *whi5* mutants) dots correspond to Nam-responsive mutants. The 1.23 ± 0.03 ratio (green line) was calculated from median cell volumes obtained for three independent wild-type cultures. Note that the origin of both axes is set at 25 fl. (**B** and **C**) Mutation in either *RPL35B* or *RAP49* genes is epistatic to *sir2*. Characteristic volume distributions were obtained on wild-type and mutant strains grown as in Figure 1A. Insets correspond to the mean of median cell volumes measured on at least four independent cultures. Error bars indicate variation to the mean.

and *rpa49* (Figure 2C), and found that both mutants were fully epistatic to *sir2* and, hence, presumably act downstream of Sir2 in the pathway. Another set of 74 mutants responded to Nam similar to wild-type cells (1.18 < Nam treated/untreated ratio < 1.28), indicating that the mutated gene and the Nam treatment probably act through independent means on cell size control. Interestingly, most of these mutants (42/74, P-value $= 3.6 \times 10^{-13}$) affected various components of mitochondria (Supplementary Table 2). In addition to these fully responsive and unresponsive mutants, the remaining 93 mutants behaved in an intermediary way (54/93; 1.05 < Nam treated/untreated ratio < 1.18) or appeared hyper-responsive to Nam (39/93; Nam treated/untreated ratio > 1.28; Supplementary Table 2). This reveals complex gene/gene relationships that cannot be easily arranged into a pathway but may, in the future, be informative to understand the whole network.

Strikingly, most of the Nam-unresponsive mutants (18/22) corresponded to knockout of genes encoding proteins implicated in diverse ribosome biogenesis steps (Supplementary Table 1). This was confirmed by GO term analyses (Supplementary Table 2) revealing a very significant enrichment for components of the cytosolic ribosome (13/22; P-value $= 2.2 \times 10^{-14}$) and more specifically cytoplasmic large ribosomal subunit (10/22; P-value $= 3.5 \times 10^{-12}$). In addition to the intrinsic constituents of the ribosome, six other proteins affected in the NAM-unresponsive mutants are involved in rRNA synthesis/maturation (Pih1, Uaf30 and Rpa49), or required for ribosome assembly (Yvh1, Zuo1 and Jjj1). Finally, we noticed that for two mutants, *bud19* and *ygr160w*, the deletion of the coding region affected overlapping genes, namely *RPL39* and *NSR1*, both required for ribosome synthesis. Hence, our pharmaco-epistasis analysis revealed a very strong enrichment for cytosolic ribosome mutants, although, quite surprisingly, strains deleted for two major ribosome biogenesis regulators, namely *sfp1* or *sch9* (Jorgensen *et al*, 2002; Jorgensen *et al*, 2004), were fully responsive to Nam (Figure 2A, blue dots), indicating that Sfp1 and Sch9 affect cell size mostly independently of Sir2.

To get a more complete view of the role of the ribosome in cell size homeostasis, we measured the volume of every non-essential ribosomal protein mutants. Most of the yeast genes encoding ribosomal proteins are duplicated and, therefore, knockout of one of the two gene copies is generally not lethal. This analysis revealed a strong bias among ribosomal protein mutants: knockout of most of the large ribosomal subunit (60S) genes resulted in a Whi phenotype, whereas small subunit (40S) mutant cells were generally larger than wild-type cells (Figure 3A and Supplementary Table 3). It should be stressed that for each ribosomal protein, the respective contribution of the two copies can be different. Therefore, for most of the mutants, the absence of a major cell volume phenotype could just reflect a minor contribution of the mutated gene copy. In any case, the cell volume distribution between 40S and 60S mutants was significantly different (Figure 3B) as previously observed by Hoose *et al* (2012), although in their study the significance of the difference between the two subunits was lower.

The opposite effects of small- and large-subunit mutants on cell size may either reflect antagonistic impacts on the same
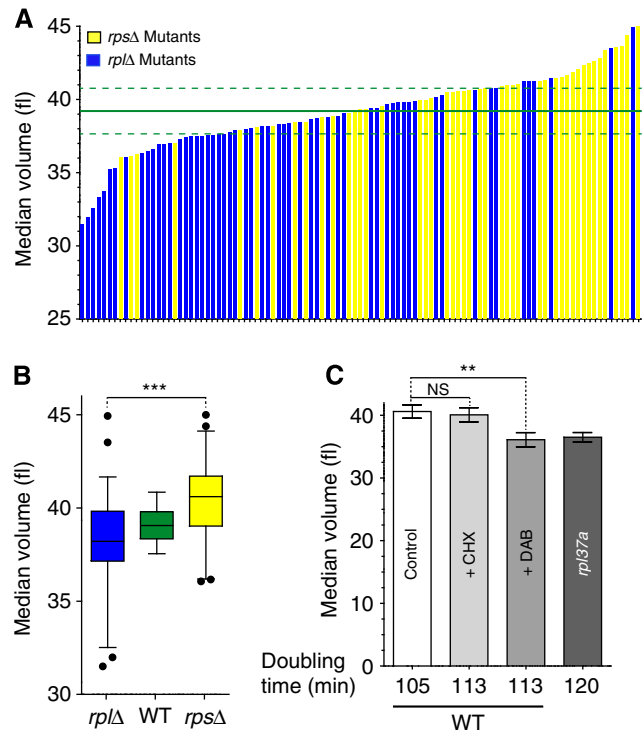

Figure 3 Impairment of small and large ribosomal subunits differentially affects cell size homeostasis. (**A**) Histogram of median cell volumes measured for mutants of the small (yellow, *rps*Δ) or the large (blue, *rpl*Δ) ribosomal subunits (see Supplementary Table 3 for details). Green lines correspond to the wild-type mean of median cell volume (plain line) and the corresponding variation to the mean (dashed lines). (**B**) Statistical analysis of median cell volume ratios obtained for 40S and 60S mutants. The statistical analysis corresponds to a Wilcoxon test with 95% confidence intervals (***$P < 10^{-4}$; GraphPad Prism). Wild-type median cell volumes were determined for 10 independent cultures. (**C**) DAB treatment affecting the large ribosomal subunit biogenesis leads to a Whi phenotype. The median cell volumes of the indicated strains grown as in Figure 1 and treated for 16 h with either + DAB (0.5 mg/l) or + CHX (0.01 mg/l) are shown. Values correspond to the mean of median cell volumes measured for at least three independent cultures. Error bars indicate variation to the mean. Statistical analysis was performed using an unpaired Student's *t*-test with 95% confidence intervals (**$P < 0.003$; NS, not significantly different). The typical doubling time measured for each growth condition is shown at the bottom of the figure.

pathway or separate effects on different pathways. To address this question, we constructed double mutants combining *rpl* and *rps* mutations. These double mutants showed an intermediary phenotype, suggesting that the large and small subunits could, at least in part, act independently on cell size homeostasis (Supplementary Figure 2). Together, our results establish that the 40S and 60S ribosomal subunits do not contribute similarly to cell size homeostasis. Consistent with the genetic data, we found that diazaborine (DAB), a drug that specifically impairs 60S assembly (Pertschy *et al*, 2004), caused a decrease of wild-type cell size (Figure 3C). By contrast, the translation inhibitor cycloheximide (CHX) had no major effect (Figure 3C). Of note, in this experiment DAB and CHX were used at a low concentration, affecting only slightly and similarly the generation time (Figure 3C).

Together, these data point to an important role for the large ribosomal subunit in cell size homeostasis, most probably downstream of Sir2. It should be noted that those cell size
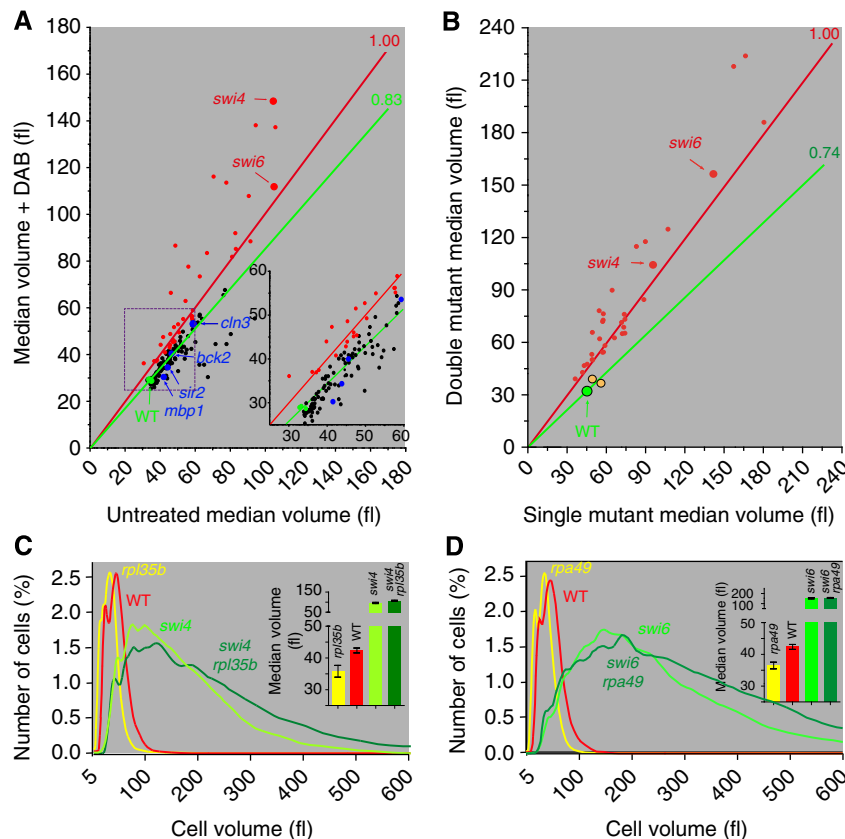
Figure 4 Identification of the Sir2–60S pathway downstream effectors. (**A**) Identification of the DAB-insensitive large (*lge*) mutants. Median cell volume were obtained on *lge* mutants kept in exponential phase of growth for 36 h in SDcasaU and then treated (*y* axis) or not (*x* axis) for 16 h with DAB (0.5 mg/l). Red dots correspond to unresponsive mutants (median cell volume ratio + DAB/ − DAB > 0.95), whereas green (WT), black (*lge* mutants) and blue (*bck2*, *cln3*, *mbp1*, and *sir2*) dots correspond to mutants differently responsive to DAB. The 0.83 ± 0.02 ratio (green line) was calculated from median cell volumes obtained from four independent wild-type cell cultures. Inset corresponds to a zoom of the region between 25 and 60 fl on both axes (purple dashed rectangle). (**B**) Validation of the DAB-unresponsive mutants by genetic epistasis relationships. Double (*y* axis) and single (*x* axis) mutants, respectively, refer to strains containing the DAB-unresponsive candidate mutations combined or not with the *rpa49::HIS3* mutation. Median cell volumes of single and double mutants were determined on cells kept in exponential phase of growth for 24 h in SDcasaU medium (see Supplementary Table 5 for more details). Control (*RPA49* (*x* axis) and *rpa49::HIS3* (*y* axis)) and false-positive strains (see text) correspond to the green and orange dots, respectively. The 0.74 ± 0.08 ratio (green line) was calculated from median cell volumes obtained on three independent cultures of wild-type and *rpa49* strains. (**C** and **D**) Validation by classical epistasis of the downstream role of Swi4 or Swi6 in the Sir2/60S controlling pathway. Characteristic volume distributions were obtained on wild-type and mutant strains grown as in Figure 1A. Insets correspond to the mean of median cell volumes measured on at least four independent cultures. Error bars indicate variation to the mean.

mutants affect various steps of 60S synthesis and/or assembly, which take place in specific cellular compartments, suggesting that it is the assembled 60S particle rather than an intermediary assembled step that is important for cell size regulation.

Swi4 and Swi6 act in the downstream part of the Sir2–60S pathway

To further progress in our understanding of the genetic network involved in the Sir2/60S cell size control pathway, we again used a pharmaco-epistasis approach. A set of 155 large mutants (corresponding to the largest mutants without major growth defect among those identified by Tyers and coworkers (Jorgensen *et al*, 2002)) were treated with DAB, which impairs 60S assembly and decreased cell size (Figure 3C). This allowed us to identify DAB-unresponsive mutants, potentially acting downstream of the Sir2/60S part of

the pathway (Figure 4A). As the wild-type cell median volume ratio was 0.83 ± 0.02, we considered as unresponsive the 40 mutants showing a ratio treated/untreated > 0.95 (red dots in Figure 4A and Supplementary Table 4). To validate the pharmaco-epistasis approach, we used classical genetics to combine each of the 40 unresponsive mutants with the *rpa49* deletion, resulting in a robust Whi phenotype insensitive to Nam (Figure 2A) and epistatic to *sir2* (Figure 2C). Among them, 33 were clearly epistatic to *rpa49* (Figure 4B, red dots and Supplementary Table 5) fully validating the pharmaco-epistasis results, 2 were hypostatic and were considered as false positive (i.e., not confirmed by classical genetics; orange dots in Figure 4B and Supplementary Table 5) and 5 double mutants could not be obtained (Supplementary Table 4). GO term analysis on the 33 confirmed mutants did not reveal any strong enrichment for a given cell component or function (Supplementary Table 6) that would give a clue on how the Sir2/60S pathway impinge on cell size. However, our attention was particularly drawn on *swi4* and *swi6*, the subunits of the
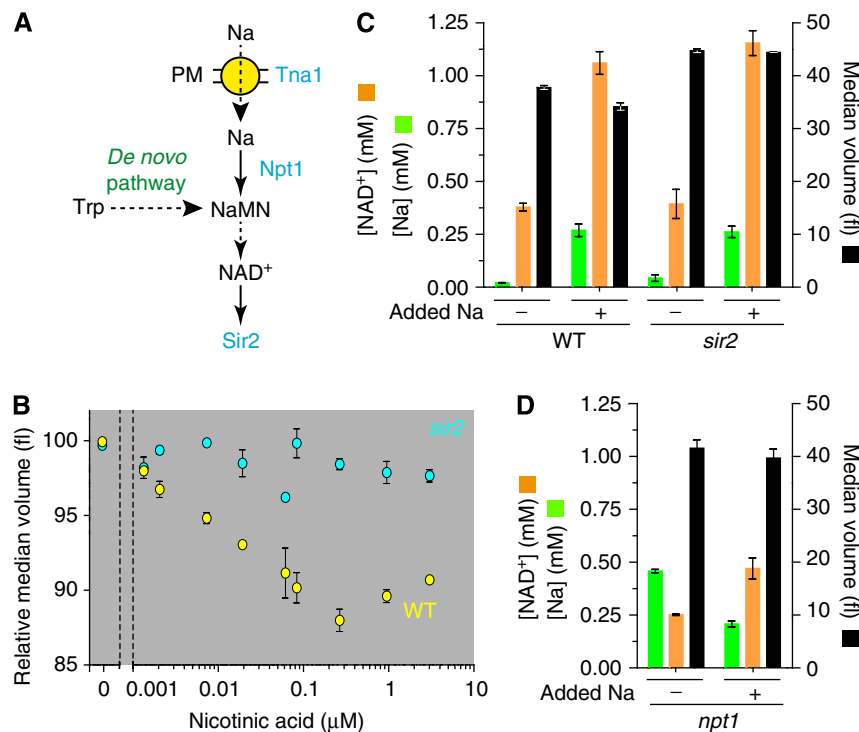
Figure 5 Control of cell size by the Sir2/60S pathway respond to NAD$^+$ variations. (**A**) Schematic representation of NAD$^+$ synthesis and salvage pathways. Na, nicotinic acid (Niacin or vitamin B3); NAD$^+$, β-NAM adenine dinucleotide; Nam, nicotinamide; NaMN, β-Na adenine mononucleotide; PM, plasma membrane. Protein names are in blue. (**B**) Na affects median volume of wild-type but not of *sir2* cells. Wild-type (BY4742) and *sir2* strains kept in exponential phase for 48 h in SDcasaU Na-free medium supplemented with different concentrations of Na (from 0 to 3 μM). For each strain, the median volume measured in the absence of external Na was used as reference. (**C** and **D**) Intracellular NAD$^+$ (orange bars) and Na (green bars) concentrations in wild type, *sir2* and *npt1* strains. Cells were kept in exponential phase for 48 h in SDcasaU Na-free medium containing or not external Na (added Na, 3 μM). Median volumes are shown in black. Metabolites were extracted and separated by liquid chromatography as described in the Materials and Methods section. Results presented in **B**–**D** correspond to the mean of at least three independent cultures for each condition and error bars indicate the variation to the mean.

SBF complex (see Introduction section). We first verified that *swi4* and *swi6* mutants were fully epistatic to *rpa49*, *rpl35b* or *rpl37a* knockout (Figure 4C and D and Supplementary Figure 3A and B). As SBF (Swi4–Swi6) and MBF (Swi6–Mbp1) are known to act downstream of Cln3 and Whi5 in cell size control, we wished to examine how DAB affected cell size of these mutants. By contrast to *swi4* and *swi6*, the *mbp1* mutant showed a wild-type cell size and was highly responsive to DAB (Figure 4A, blue dot). This result indicates that the SBF complex, but not the MBF complex, is required downstream of the Sir2–60S pathway. Unlike *swi4* and *swi6*, the *cln3* or *bck2* mutants deleted for the upstream effectors were responsive to DAB (Figure 4A, blue dot). Together, these pharmaco-epistasis analyses strongly suggest that Swi4 and Swi6 are positioned in the downstream portion of the Sir2/60S pathway, independently to their known upstream effectors (Cln3, Bck2 and Whi5).

NAD$^+$ as a physiological signal modulating cell size through the Sir2/60s pathway

Our results establish that Sir2 and the 60S subunit define a new pathway that contributes to cell size homeostasis. We subsequently questioned the nature of the physiological signals that would modify Sir2 activity and thereby regulate

cell size homeostasis. Sir2 activity is known to be modulated by NAD$^+$ (Imai *et al*, 2000; Landry *et al*, 2000), which can be either synthesized *de novo* from tryptophan or recycled from Na (Figure 5A; Kucharczyk *et al*, 1998; Bieganowski and Brenner, 2004). Feeding wild-type cells with increasing concentrations of Na resulted in a progressive cell size decrease (Figure 5B, yellow dots). As expected, Na addition also caused a drastic increase in cellular NAD$^+$ in both wild-type and *sir2*Δ cells (Figure 5C). However, although Na treatment affected wild-type cell size, this was not the case for the *sir2*Δ mutant (Figure 5B, blue dots). Importantly, a *npt1* mutant that is impaired for synthesis of NAD$^+$ from Na was large and did not respond to extracellular Na (Figure 5D, black bars). In this mutant, intracellular Na concentration was high and NAD$^+$ concentration was low compared with wild type (Figure 5D), as expected if the recycling of Na to NAD$^+$ is impaired. Together, these results point to NAD$^+$, or a derivative, as a physiological signal that regulates the Sir2/60S pathway. As NAD$^+$ is thought to be the natural activator of Sir2 (Imai *et al*, 2000) and as *sir2*Δ cells are unresponsive to Na and NAD$^+$ variations (Figure 5C), we conclude that NAD$^+$ is a very strong candidate as a metabolic regulator of cell size in yeast. We thus propose that Sir2 contributes to the control of cell size homeostasis in yeast in response to variations of the NAD$^+$ intracellular pool.
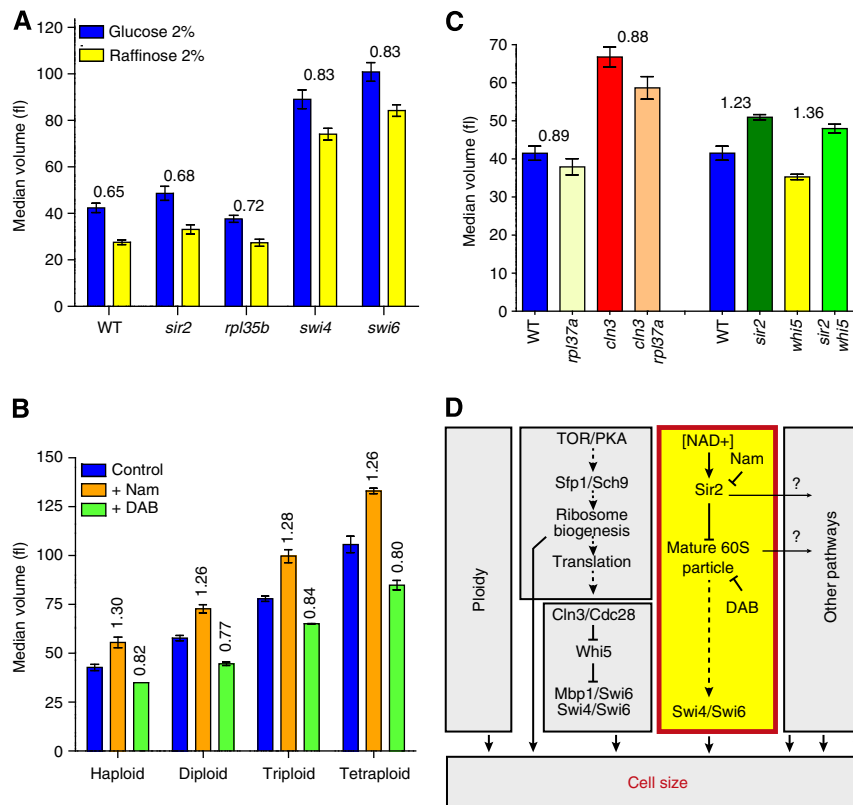
Figure 6 The Sir2/60S pathway mutants still respond to nutritional control and ploidy effects on cell size. (**A**) Cells were kept in exponential phase for 48 h in SDcasaU or SRafcasaU media. Results correspond to the mean of median cell volumes obtained for at least three independent cultures. Error bars indicate variation to the mean. Median volume ratios using glucose as a reference are indicated. (**B**) Cells with various ploidies were grown in SDcasaU and treated as in **A**. Median cell volume ratios are indicated using untreated cells as a reference. (**C**) Sir2/60S pathway modulates cell size independently of the Cln3/Whi5 effectors. Cells were kept in exponential phase for 48 h in SDcasaU media. Results correspond to the mean of median cell volumes obtained for at least four independent cultures and error bars indicate variation to the mean. (**D**) Schematic representation of the role of the sir2/60S pathway in the cell size controlling network.

Positioning of the Sir2/60S pathway in the cell size control network

To get a more global view on how the Sir2/60S pathway impinges on cell size control in yeast, we examined the connections between known yeast cell size regulations and the Sir2/60S pathway. Cell size, similar to most complex traits, is not only affected by multiple genes but also by the environment and particularly by the richness of the growth medium. As an example, wild-type yeast cells grown in the presence of raffinose, a carbon source less efficiently metabolized than glucose, have a $35\% \pm 4$ reduced cell volume (Figure 6A). Importantly, carbon source control of cell size was still active in the Sir2/60S pathway mutants (Figure 6A). Yet, the most downstream mutants, *swi4* and *swi6*, which are not specific to the Sir2/60s pathway, are less, although still significantly, affected by nutrients than wild-type cells (Figure 6A). We conclude that the Sir2/60S pathway acts on cell size homeostasis independently of the raffinose/glucose nutritional control.

In our attempt to place the Sir2/60S pathway in a more global network resulting in cell size homeostasis, we also evaluated the relationships between the Sir2/60S pathway and ploidy. As previously shown (Galitski *et al*, 1999), we found that cell size increased with ploidy (Figure 6B). Yet, whatever

the ploidy, a Nam treatment resulted in a $27 \pm 3\%$ increase of cell size, whereas DAB led to a $19 \pm 4\%$ decrease (Figure 6B). From these results, we conclude that the Sir2/60S pathway and the ploidy control of cell size are not linked.

Finally, we confirmed by classical genetics (Figure 6C) the pharmaco-epistasis relationships found for *whi5* (i.e., responsive to Nam; Figure 2A, blue dot) and *cln3* (i.e., responsive to DAB; Figure 4A, blue dot). These results imply that the Sir2/60S pathway modulates cell size independently of the Cln3/Whi5 pathway, although both pathways have Swi4 and Swi6 in common (Figure 6D).

Mutations in *SIR2* and 60S genes affect both cell size and replicative life span but the two phenomena are not strictly interdependent

It is noteworthy that Sir2 is a major factor of the yeast replicative aging, a process defined as the number of successive daughters produced by a cell before becoming senescent (Kaeberlein *et al*, 1999). In addition, a specific behavior for 60S ribosomal subunit mutants was previously reported in yeast for other phenotypes, including replicative aging (Steffen *et al*, 2008). The fact that *SIR2*, 60S mutants, medium richness and cell ploidy all affect both replicative
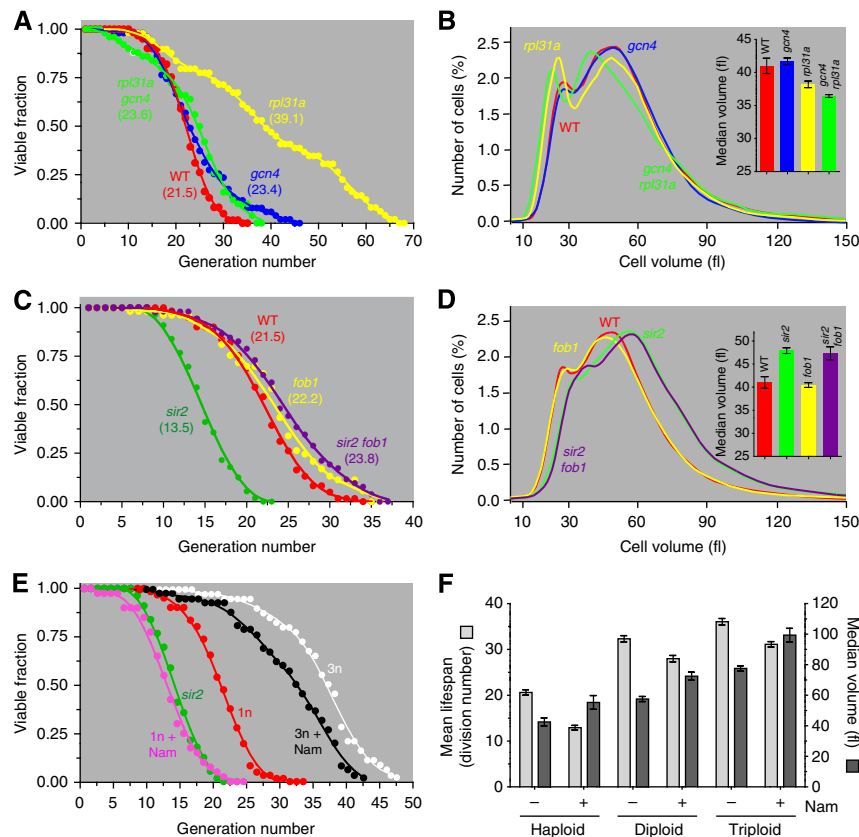
Figure 7 Sir2/60S pathway affects both cell size and replicative life span, but the two pathways can be disconnected. (**A** and **B**) Deletion of *GCN4* suppresses the replicative life span phenotype (**A**) but not the cell volume phenotype (**B**) of the *rpl31a* mutant. Survival curves were determined twice on at least 50 daughters of daughter cells on solid YPD medium. For each strain, the mean replicative life span is indicated in brackets. Median cell volume measurements were determined on cells grown as in Figure 1A. (**C** and **D**) Knockout of *fob1* suppresses the replicative life span phenotype (**C**) but not the cell size phenotype (**D**) of the *sir2* mutant. (**E** and **F**) Effect of both ploidy and Nam treatment on wild-type cells replicative life span and volume. Survival curves (**E**) were determined twice on 50–100 daughters of daughter cells for each strain grown on YPD medium containing or not Nam (500 μM). (**F**) Effect of Nam on replicative life span (light gray) and median cell volume (dark gray) of wild-type cells of various ploidies.

aging and cell size homeostasis provocatively suggests that the two phenomena may be linked as previously proposed by others (Yang *et al*, 2011). To directly address this longstanding issue, we used combinations of mutations known to differently affect replicative life span. As reported previously, we found a clear increase in the generation number for the *whi* mutant *rpl31a* (Figure 7A; Steffen *et al*, 2008). However, the *gcn4* deletion, suppressing the *rpl31a* replicative life span increase (Figure 7A; Steffen *et al*, 2008), had no effect on the *rpl31a* Whi phenotype (Figure 7B). Similarly, the *fob1* mutation, which suppresses the *sir2* replicative life span defect (Figure 7C; Kaeberlein *et al*, 1999), did not suppress the large phenotype of *sir2* (Figure 7D). Finally, as previously observed, Nam decreased replicative life span (Bitterman *et al*, 2002) and this effect was found independent of the cell ploidy, as expected if it mimics a Sir2 defect (Figure 7E and F). However, replicative life span of untreated diploid and triploid cells was longer than that of haploid cells, despite the fact that increased ploidy resulted in an increased cell size (Figures 6C, and 7E and F). Consequently, higher ploidy and Nam treatment of a wild-type strain both increased cell size but had opposite effects on replicative life span. We thus conclude that cell size and replicative life span, although affected by a common set of mutants, can be disconnected.

Discussion

Cell size, a highly complex trait regulated by hundreds of genes, offers a challenging framework to explore how complex genetic information is integrated in a phenotypic outcome. The understanding of such a complex network requires the identification of all the participating genes and the precise measurement of their individual and concerted contribution to the phenotype. These complex interactions between genes are referred to as epistasis, in the widest sense of the term. In yeast, epistasis is classically monitored after combining the mutations to be studied by mating and sporulation. This can be done on a large scale using approaches developed for SGAs (Tong *et al*, 2001). However, it still requires mating and sporulation, which take time, and may be difficult in some specific cases such as for *sir2* mutants, which are mating deficient. Here we used a pharmaco-epistasis approach based on the use of inhibitors to mimic specific mutations and thereby perform large-scale epistasis analyses. To restrict possible off-target effects, this approach needs the use of as low as possible concentrations of inhibitors, and when possible it should be validated by classical genetics. A major advantage of pharmaco-epistasis is that as no meiosis is required, the phenotype comparison is done on strictly

identical individuals in terms of genotype. Simple epistasis relationships are observed when one mutation (or drug mimicking the mutation) masks the effects of another mutation. We first concentrated on these situations, because they are relatively easy to interpret and allow positioning genes into linear regulatory pathways.

In the case of cell size control, we benefit from the large set of data provided by Tyers and coworkers (Jorgensen *et al*, 2002). We started from a set of knockout mutants showing the most extreme Whi (189 mutants) or Lge (155 mutants) phenotypes. It should be stressed that there is no theoretical reason to choose the most affected mutants, but this choice relies mainly on practical reasons. Indeed, measuring precisely cell size on multiple different yeast strains is a technically challenging issue (Turner *et al*, 2012). Accordingly, in the course of this work, we observed that cell size is exquisitely sensitive to growth conditions. Even though we paid a particular attention to this point, the experimental error is routinely $\pm 5\%$. Consequently, it is much easier and it raises much stronger conclusions, in terms of statistical significance, to study combinations of mutants with extreme phenotypes.

We identified a subset of >50 genes belonging to a new cell size homeostasis pathway (Figure 6D). Remarkably, this pathway includes numerous mutants affecting ribosome biogenesis and more specifically the large ribosomal subunit. Of note, it would not be surprising that *sir2* affects cell size homeostasis through its effect on silencing of rDNA (Smith and Boeke, 1997). Previous work from Tyers and coworkers (Jorgensen *et al*, 2004) had established a strong connection between ribosome biogenesis and cell size homeostasis. Here we observed that small ribosomal subunit mutants tend to be larger than the wild-type control cells, whereas large ribosomal subunit mutants are often Whi. In addition, combination of 40S and 60S mutants resulted in an intermediary phenotype, strongly suggesting that these mutants affect cell size homeostasis by different mechanisms. It thus appears that there is not just one connection between ribosome biogenesis and cell size homeostasis but several layers of control. The first layer involves the Sfp1 and Sch9 effectors on the *Ribi* and *RP* regulons that connect nutrient control to critical size via the rate of ribosome production (Jorgensen *et al*, 2004). Our data establish that the Sir2/60S pathway is clearly distinct from the Sfp1/Sch9 network. First, as both *sfp1* and *sch9* mutants are fully responsive to Nam, and second, as Sir2/60S mutants are responsive to nutrients, whereas *sfp1* or *sch9* mutants are not (Jorgensen *et al*, 2004). However, the *swi4* and *swi6* mutants, the most downstream components of the pathway, although less responsive to the carbon source than wild-type, are not fully insensitive (Figure 6A). This suggests that these components integrate regulatory signals from separate pathways (Figure 6D). A second layer of ribosomal effect on cell size involves the translational control of Cln3 (Polymenis and Schmidt, 1997). Yet, it is striking that Cln3 is neither required for ploidy control (Andalis *et al*, 2004) nor for nutrient control (Jorgensen *et al*, 2004) or the Sir2/60S pathway (this work). Further studies will be required to position Cln3 in the cell size homeostasis control network. The third layer, revealed by our pharmaco-epistasis study, specifically involves the 60S ribosomal subunit. Intriguingly, a specific behavior of 60S mutants was previously reported in yeast for other phenotypes such as

ER stress response (Miyoshi *et al*, 2002; Zhao *et al*, 2003) or replicative aging (Steffen *et al*, 2008). However, in both cases the underlying molecular mechanisms remain largely unknown.

In addition to the simple epistasis relationships, more complex gene/gene interactions were found, which cannot be simply interpreted. For instance, many mutants showed an intermediary response to Nam, indicating that they are not fully responsive to Nam but are neither totally irresponsive. Interestingly, among the 54 mutants behaving this way, more than half affected cytosolic ribosome. How should we interpret these partial effects? First, despite the fact that the mutants used in this study are knockout, some effects could be partial due to gene redundancy; this is clearly the case for ribosomal protein genes that are generally duplicated. Second, some gene interactions can be more complicated than just phenotypic masking. In particular, it is likely that many of the studied mutants have pleiotropic effects that could simultaneously affect more than one pathway. In this type of analyses, one should keep in mind the multiple levels of complexity due to allelic diversity and specificity. In this perspective, yeast offers a simplified model due to the possible use of knockout mutations and to the fact that the genetic network is analyzed in haploid cells.

Another major level of complexity is interaction between genetic factors and the environment. Once again, yeast, as it is a unicellular organism, provides a simpler experimental frame. Strikingly, we found that the abundance of the coenzyme NAD^+ appears as a major regulator of cell size homeostasis. Abundance of free NAD^+ results from *de novo* synthesis and recycling from precursors such as Na, but also from its equilibrium with the reduced NADH form. It has been shown that in living cells, free NAD^+ is several orders of magnitude more abundant than free NADH (Williamson *et al*, 1967; Zhang *et al*, 2002b). NAD^+ concentration in yeast has been estimated to be in the millimolar range (Belenky *et al*, 2007; this work). This concentration is by far higher than the Km of Sir2 for NAD^+, which is about $30\,\mu M$ (Bedalov *et al*, 2003; Borra *et al*, 2004). Consequently, it seems likely that activation of Sir2 by NAD^+ does not simply reflect substrate availability but more probably relies on a more complex regulatory mechanism involving allosteric effects. Accordingly, our results show that moderate variations of NAD^+ concentration may impinge on cell size. Through its role in regulating Sir2 activity, we propose that NAD^+ acts as a 'metabolic cell sizer,' providing a simple and efficient mechanism to adapt cell size to metabolic status.

Finally, the discovery of the Sir2/60S pathway as a major factor in cell size homeostasis echoed its effect on replicative aging (Steffen *et al*, 2008), raising the hypothesis of a causal connection between cell size and aging. In addition, as noticed by Schneider and coworkers (Yang *et al*, 2011), many cell size mutants are also affected for replicative life span. Accordingly, growth under conditions where carbon is limiting results in a decreased cell size and an increased replicative life span. However, we showed here that Fob1 and Gcn4, which are clearly involved in the replicative aging process, do not affect cell size, thus disconnecting the two phenomena. Moreover, both the treatment of cells with Nam and an increased ploidy resulted in a larger median cell volume, while having opposite

effects on replicative life span. Hence, it seems that no simple connection between the two phenomena can yet be drawn. A similar conclusion was reached by Guarente and coworkers (Kennedy *et al*, 1994) on yeast cells artificially enlarged by α-factor arrest, although opposite results have also been reported (Zadrag *et al*, 2005). At this point, it is not possible to draw a definitive conclusion on this complex relationship between cell size and aging. Indeed, although many signaling pathways are shared by cell size and longevity, suggesting important common mechanisms, conspicuous counter examples such as those reported in this work rather argue for a disconnection of the two phenomena. The fascinating question of relationships between size and life span of living organisms rose by Aristotle in his essay 'On Longevity and Shortness of Life' 23 centuries ago, remains open.

Materials and methods

Media, strains and plasmids

SDcasaU is a synthetic minimal medium containing 5% ammonium sulfate, 0.67% yeast nitrogen base (Difco) and 2% glucose, supplemented with 0.2% casamino acids (Difco) and uracil (0.3 mM). SRafcasaU is a similar medium containing 2% raffinose instead of glucose. In specific experiments requiring modulation of Na concentrations, SDcasaU was made with Na-free yeast nitrogen base (Formedium) and was supplemented with indicated concentrations of Na (Sigma-Aldrich). The YPD medium used for replicative life span experiments contained 1% yeast extract, 2% peptone, 2% glucose. NAM (Sigma-Aldrich) and DAB (kind gift from Dr H Bergler) were used at indicated concentrations. All yeast strains were derived from the parent strains BY4741 and BY4742 of the haploid yeast ORF deletion collections (Winzeler *et al*, 1999). Polyploid strains isogenic to BY4741 and BY4742 strains were obtained from David Pellman (Storchova *et al*, 2006). The *rpa49*::*HIS3* mutants were obtained by transformation of wild-type or single mutant strains with a PCR fragment obtained on genomic DNA from the SL107-3B strain (Beckouet *et al*, 2008; generous gift from Michel Werner) with oligonucleotides RPA49up (5′-CGACG CCAATTAGCAATACTG-3′) and RPA49Rv (5′-CTATTTGTACATATGTATC TTCTCAG-3′). Histidine-prototrophic transformants were selected and insertion of the *rpa49*::*HIS3* cassette at *RPA49* locus was verified by PCR with oligonucleotides RPA49prom (5′-TTCTTTAGCTTGTGGCG TTGG-3′) and RPA49Rv. All other multiple mutant strains used in this study were obtained by mating, sporulation and tetrad dissection. Double mutants were identified by PCR using the KanB oligonucleotide (internal to KanMX4; 5′-CTGCAGCGAGGAGCCGTAAT-3′) and an oligonucleotide complementary to the promoter of the disrupted gene. The *sir2* mutation leading to a decreased mating efficiency (Shore *et al*, 1984), construction of double mutants was also done by crossing, but with a *sir2* mutant strain covered by a *SIR2* centromeric plasmid (p4099; *URA3*; lab collection). Meiotic *sir2* segregants, having lost the plasmid, were then identified as uracil auxotroph. Doubling time of the most used strains in this study are as follows: wild-type strain (105 min), *rpl31a* (120 min), *rpl35b* (130 min), *rpa49* (135 min), *sir2* (105 min), *swi4* (165 min) and *swi6* (165 min).

Cell size distribution measurements

All cell size measurements were performed by determining the median cell volume of asynchronous yeast cell cultures using a Coulter-counter apparatus (Beckman-Coulter). Compared with other methods used for yeast cell volume measurement, this method is fast and accurate, and allows to process multiple samples (Turner *et al*, 2012). Cells were grown overnight in SDcasaU or SRaffcasaU media, and then diluted several times in order to maintain exponential growth (cell number is always kept under 2×10^7 cells/ml) for 24–48 h before cell size measurement. It should be stressed that we noticed a significant effect of culture conditions on wild-type cell volume (Supplementary Figure 4). Consequently, volume comparisons

require to be done on cells grown in the exact same conditions. To obtain each cell size distribution, 100 μl of culture were then diluted into 10 ml of IsotonII (Beckman-Coulter) and size distribution of the population was analyzed with a multisizer4 (Beckman-Coulter) by counting between 10 000 and 20 000 cells for each measurement. Results are given as the percentage of cells counted in each of the 400-size classes. Median volume was obtained from the geometric cell volume distribution by using the Multi4 software (4.02 version; Beckman-Coulter) with a smoothing of 7 as previously done in yeast (Jorgensen *et al*, 2002). Statistical significance of differences between two conditions has been determined through the use of an unpaired Student's *t*-test (Graphpad Prism Software). For size determination in presence of Nam (100 μM), DAB (0.5 mg/l) and CHX (0.01 mg/l), cells were incubated in the presence of the indicated drugs for 8 h (Nam) or 16 h (DAB and CHX) before measurements. For epistasis studies, median cell volumes were determined on the four spores of at least four tetratypes.

Replicative life span analysis

All replicative life span experiments were carried out (at least twice) as described (Kaeberlein *et al*, 2005) on 50–100 daughters of daughter cells grown on standard YPD plates containing or not Nam (500 μM, a dose resulting in a 20% median volume increase on plates). Statistical significance of replicative life span changes between strains was determined using a Wilcoxon rank-sum test (GraphPad Prism Software) using a cutoff value of $P = 0.05$.

Intracellular metabolites determination

Wild-type and mutant strains were kept in exponential phase for 48 h in SDcasaU Na-free medium supplemented or not with extracellular Na (3 μM, corresponding to the concentration found in Na-containing SD medium). Metabolites extraction by rapid filtration and ethanol boiling method, and metabolite separation by liquid chromatography were performed as described previously (Hurlimann *et al*, 2011; Laporte *et al*, 2011).

Supplementary information

Supplementary information is available at the *Molecular Systems Biology* website (www.nature.com/msb).

Conflict of interest

The authors declare that they have no conflict of interest.

References

Adams J, Hansche PE (1974) Population studies in microorganisms. I. Evolution of diploidy in *Saccharomyces cerevisiae*. *Genetics* **76**: 327–338

Andalis AA, Storchova Z, Styles C, Galitski T, Pellman D, Fink GR (2004) Defects arising from whole-genome duplications in *Saccharomyces cerevisiae*. *Genetics* **167**: 1109–1121

Beckouet F, Labarre-Mariotte S, Albert B, Imazawa Y, Werner M, Gadal O, Nogi Y, Thuriaux P (2008) Two RNA polymerase I subunits control the binding and release of Rrn3 during transcription. *Mol Cell Biol* **28**: 1596–1605

Bedalov A, Hirao M, Posakony J, Nelson M, Simon JA (2003) NAD + -dependent deacetylase Hst1p controls biosynthesis and cellular NAD + levels in *Saccharomyces cerevisiae*. *Mol Cell Biol* **23**: 7044–7054

Belenky P, Racette FG, Bogan KL, McClure JM, Smith JS, Brenner C (2007) Nicotinamide riboside promotes Sir2 silencing and extends lifespan via Nrk and Urh1/Pnp1/Meu1 pathways to NAD + . *Cell* **129**: 473–484

Bieganowski P, Brenner C (2004) Discoveries of nicotinamide riboside as a nutrient and conserved NRK genes establish a Preiss-Handler independent route to NAD + in fungi and humans. *Cell* **117**: 495–502

Bitterman KJ, Anderson RM, Cohen HY, Latorre-Esteves M, Sinclair DA (2002) Inhibition of silencing and accelerated aging by nicotinamide, a putative negative regulator of yeast sir2 and human SIRT1. *J Biol Chem* **277**: 45099–45107

Borra MT, Langer MR, Slama JT, Denu JM (2004) Substrate specificity and kinetic mechanism of the Sir2 family of NAD + -dependent histone/protein deacetylases. *Biochemistry* **43**: 9877–9887

Carter BL, Sudbery PE (1980) Small-sized mutants of *Saccharomyces cerevisiae*. *Genetics* **96**: 561–566

Costanzo M, Nishikawa JL, Tang X, Millman JS, Schub O, Breitkreuz K, Dewar D, Rupes I, Andrews B, Tyers M (2004) CDK activity antagonizes Whi5, an inhibitor of G1/S transcription in yeast. *Cell* **117**: 899–913

de Bruin RA, McDonald WH, Kalashnikova TI, Yates 3rd J, Wittenberg C (2004) Cln3 activates G1-specific transcription via phosphorylation of the SBF bound repressor Whi5. *Cell* **117**: 887–898

Ferrezuelo F, Aldea M, Futcher B (2009) Bck2 is a phase-independent activator of cell cycle-regulated genes in yeast. *Cell Cycle* **8**: 239–252

Galitski T, Saldanha AJ, Styles CA, Lander ES, Fink GR (1999) Ploidy regulation of gene expression. *Science* **285**: 251–254

Goranov AI, Amon A (2010) Growth and division–not a one-way road. *Curr Opin Cell Biol* **22**: 795–800

Goranov AI, Cook M, Ricicova M, Ben-Ari G, Gonzalez C, Hansen C, Tyers M, Amon A (2009) The rate of cell growth is governed by cell cycle stage. *Genes Dev* **23**: 1408–1422

Guarente L (1999) Diverse and dynamic functions of the Sir silencing complex. *Nat Genet* **23**: 281–285

Hartwell LH, Culotti J, Pringle JR, Reid BJ (1974) Genetic control of the cell division cycle in yeast. *Science* **183**: 46–51

Harvey SL, Kellogg DR (2003) Conservation of mechanisms controlling entry into mitosis: budding yeast wee1 delays entry into mitosis and is required for cell size control. *Curr Biol* **13**: 264–275

Hennaut C, Hilger F, Grenson M (1970) Space limitation for permease insertion in the cytoplasmic membrane of *Saccharomyces cerevisiae*. *Biochem Biophys Res Commun* **39**: 666–671

Hoose SA, Rawlings JA, Kelly MM, Leitch MC, Ababneh QO, Robles JP, Taylor D, Hoover EM, Hailu B, McEnery KA, Downing SS, Kaushal D, Chen Y, Rife A, Brahmbhatt KA, Smith 3rd R, Polymenis M (2012) A systematic analysis of cell cycle regulators in yeast reveals that most factors act independently of cell size to control initiation of division. *PLoS genetics* **8**: e1002590

Hurlimann HC, Laloo B, Simon-Kayser B, Saint-Marc C, Coulpier F, Lemoine S, Daignan-Fornier B, Pinson B (2011) Physiological and toxic effects of purine intermediate 5-amino-4-imidazolecar-boxamide ribonucleotide (AICAR) in yeast. *J Biol Chem* **286**: 30994–31002

Imai S, Armstrong CM, Kaeberlein M, Guarente L (2000) Transcriptional silencing and longevity protein Sir2 is an NAD-dependent histone deacetylase. *Nature* **403**: 795–800

Johnston GC, Ehrhardt CW, Lorincz A, Carter BL (1979) Regulation of cell size in the yeast *Saccharomyces cerevisiae*. *J Bacteriol* **137**: 1–5

Johnston GC, Pringle JR, Hartwell LH (1977) Coordination of growth with cell division in the yeast *Saccharomyces cerevisiae*. *Exp Cell Res* **105**: 79–98

Jorgensen P, Nishikawa JL, Breitkreutz BJ, Tyers M (2002) Systematic identification of pathways that couple cell growth and division in yeast. *Science* **297**: 395–400

Jorgensen P, Rupes I, Sharom JR, Schneper L, Broach JR, Tyers M (2004) A dynamic transcriptional network communicates growth potential to ribosome synthesis and critical cell size. *Genes Dev* **18**: 2491–2505

Jorgensen P, Tyers M (2004) How cells coordinate growth and division. *Curr Biol* **14**: R1014–R1027

Kaeberlein M, McVey M, Guarente L (1999) The SIR2/3/4 complex and SIR2 alone promote longevity in *Saccharomyces cerevisiae* by two different mechanisms. *Genes Dev* **13**: 2570–2580

Kaeberlein M, Powers 3rd RW, Steffen KK, Westman EA, Hu D, Dang N, Kerr EO, Kirkland KT, Fields S, Kennedy BK (2005) Regulation of yeast replicative life span by TOR and Sch9 in response to nutrients. *Science* **310**: 1193–1196

Kennedy BK, Austriaco Jr NR, Guarente L (1994) Daughter cells of *Saccharomyces cerevisiae* from old mothers display a reduced life span. *J Cell Biol* **127**: 1985–1993

Kucharczyk R, Zagulski M, Rytka J, Herbert CJ (1998) The yeast gene YJR025c encodes a 3-hydroxyanthranilic acid dioxygenase and is involved in nicotinic acid biosynthesis. *FEBS Lett* **424**: 127–130

Landry J, Sutton A, Tafrov ST, Heller RC, Stebbins J, Pillus L, Sternglanz R (2000) The silencing protein SIR2 and its homologs are NAD-dependent protein deacetylases. *Proc Natl Acad Sci USA* **97**: 5807–5811

Laporte D, Lebaudy A, Sahin A, Pinson B, Ceschin J, Daignan-Fornier B, Sagot I (2011) Metabolic status rather than cell cycle signals control quiescence entry and exit. *J Cell Biol* **192**: 949–957

Lee S, Tong L, Denu JM (2008) Quantification of endogenous sirtuin metabolite *O*-acetyl-ADP-ribose. *Anal Biochem* **383**: 174–179

Lew DJ, Marini NJ, Reed SI (1992) Different G1 cyclins control the timing of cell cycle commitment in mother and daughter cells of the budding yeast *S. cerevisiae*. *Cell* **69**: 317–327

Miyoshi K, Tsujii R, Yoshida H, Maki Y, Wada A, Matsui Y, Toh EA, Mizuta K (2002) Normal assembly of 60 S ribosomal subunits is required for the signaling in response to a secretory defect in *Saccharomyces cerevisiae*. *J Biol Chem* **277**: 18334–18339

Nash R, Tokiwa G, Anand S, Erickson K, Futcher AB (1988) The WHI1 + gene of *Saccharomyces cerevisiae* tethers cell division to cell size and is a cyclin homolog. *EMBO J* **7**: 4335–4346

Pertschy B, Zisser G, Schein H, Koffel R, Rauch G, Grillitsch K, Morgenstern C, Durchschlag M, Hogenauer G, Bergler H (2004) Diazaborine treatment of yeast cells inhibits maturation of the 60S ribosomal subunit. *Mol Cell Biol* **24**: 6476–6487

Polymenis M, Schmidt EV (1997) Coupling of cell division to cell growth by translational control of the G1 cyclin CLN3 in yeast. *Genes Dev* **11**: 2522–2531

Shore D, Squire M, Nasmyth KA (1984) Characterization of two genes required for the position-effect control of yeast mating-type genes. *EMBO J* **3**: 2817–2823

Smith JS, Boeke JD (1997) An unusual form of transcriptional silencing in yeast ribosomal DNA. *Genes Dev* **11**: 241–254

Spellman PT, Sherlock G, Zhang MQ, Iyer VR, Anders K, Eisen MB, Brown PO, Botstein D, Futcher B (1998) Comprehensive identification of cell cycle-regulated genes of the yeast *Saccharomyces cerevisiae* by microarray hybridization. *Mol Biol Cell* **9**: 3273–3297

Steffen KK, MacKay VL, Kerr EO, Tsuchiya M, Hu D, Fox LA, Dang N, Johnston ED, Oakes JA, Tchao BN, Pak DN, Fields S, Kennedy BK, Kaeberlein M (2008) Yeast life span extension by depletion of 60s ribosomal subunits is mediated by Gcn4. *Cell* **133**: 292–302

Storchova Z, Breneman A, Cande J, Dunn J, Burbank K, O'Toole E, Pellman D (2006) Genome-wide genetic analysis of polyploidy in yeast. *Nature* **443**: 541–547

Sudbery PE, Goodey AR, Carter BL (1980) Genes which control cell proliferation in the yeast *Saccharomyces cerevisiae*. *Nature* **288:** 401–404

Tong AH, Evangelista M, Parsons AB, Xu H, Bader GD, Page N, Robinson M, Raghibizadeh S, Hogue CW, Bussey H, Andrews B, Tyers M, Boone C (2001) Systematic genetic analysis with ordered arrays of yeast deletion mutants. *Science* **294:** 2364–2368

Turner JJ, Ewald JC, Skotheim JM (2012) Cell size control in yeast. *Curr Biol* **22:** R350–R359

Wang CL, Landry J, Sternglanz R (2008) A yeast sir2 mutant temperature sensitive for silencing. *Genetics* **180:** 1955–1962

Weart RB, Lee AH, Chien AC, Haeusser DP, Hill NS, Levin PA (2007) A metabolic sensor governing cell size in bacteria. *Cell* **130:** 335–347

Williamson DH, Lund P, Krebs HA (1967) The redox state of free nicotinamide-adenine dinucleotide in the cytoplasm and mitochondria of rat liver. *Biochem J* **103:** 514–527

Winzeler EA, Shoemaker DD, Astromoff A, Liang H, Anderson K, Andre B, Bangham R, Benito R, Boeke JD, Bussey H, Chu AM, Connelly C, Davis K, Dietrich F, Dow SW, El Bakkoury M, Foury F, Friend SH, Gentalen E, Giaever G, Hegemann JH, Jones T, Laub M, Liao H, Davis RW *et al* (1999) Functional characterization of the *S. cerevisiae* genome by gene deletion and parallel analysis. *Science* **285:** 901–906

Wright DN, Lockhart WR (1965) Environmental control of cell composition in *Escherichia coli*. *J Bacteriol* **89:** 1026–1031

Yang J, Dungrawala H, Hua H, Manukyan A, Abraham L, Lane W, Mead H, Wright J, Schneider BL (2011) Cell size and growth rate are major determinants of replicative lifespan. *Cell Cycle* **10:** 144–155

Zadrag R, Bartosz G, Bilinski T (2005) Replicative aging of the yeast does not require DNA replication. *Biochem Biophys Res Commun* **333:** 138–141

Zhang J, Schneider C, Ottmers L, Rodriguez R, Day A, Markwardt J, Schneider BL (2002a) Genomic scale mutant hunt identifies cell size homeostasis genes in *S. cerevisiae*. *Curr Biol* **12:** 1992–2001

Zhang Q, Piston DW, Goodman RH (2002b) Regulation of corepressor function by nuclear NADH. *Science* **295:** 1895–1897

Zhao Y, Sohn JH, Warner JR (2003) Autoregulation in the biosynthesis of ribosomes. *Mol Cell Biol* **23:** 699–707